High-Strength Uniaxially Drawn Tapes from Scrap Recycled Poly(ethylene terephthalate)

J. Morawiec, Z. Bartczak, M. Pluta, A. Galeski

Centre of Molecular and Macromolecular Studies Polish Academy of Sciences, Sienkiewicza 112, Lodz, 90-363 Poland

Received 25 April 2001; accepted 7 February 2002

ABSTRACT: We made an effort to develop a manufacturing process for high-strength packaging straps from recycled poly(ethylene terephthalate) (PET) beverage bottles. High-strength tapes from low-viscosity bottle-grade PET cannot be obtained by single drawing to a natural draw ratio because the strength of such tapes is below expectation. To increase that strength, we developed a double-drawing process, consisting of a second drawing step after free drawing with the natural draw ratio. The second stretching of tapes proceeded without necking and uniformly over the entire tape length. The extrusion/stretching was performed on the laboratory line, consisting of a single screw extruder, a chill roll, two sets of slow and fast rolls separated by a heating tunnel, and wind-up roll. The tape drawn to a total draw ratio of 6 had a tensile strength slightly below 700 MPa and an initial slope of $\approx$ 15 GPa. Strain-induced crystallization was the origin of strong texture after single drawing, whereas plastic deformation mechanisms of crystals were activated in the second step of drawing: the (100)[001] chain and (100)[010] transverse slips led to clear further refining of ($\bar{1}$05) X-ray pole figure. Industrial scale up of the double drawing delivered tapes with strength slightly below 700 MPa. © 2002 Wiley Periodicals, Inc. J Appl Polym Sci 86: 1426–1435, 2002

Key words: polyesters; recycling; orientation

INTRODUCTION

Poly(ethylene terephthalate) (PET) is used commercially for a very wide range of products, including textile fibers, beverage bottles, packaging films, and moldings; it is also a base for composite materials. The amount of postconsumer scrap PET is increasing rapidly as new applications are developed and PET production grows.

There are several possibilities for recycling postconsumer scrap PET.[1–4] One of the most frequently used is the material recycling of PET beverage bottles. Regrind in the form of flakes is relatively free of impurities, and the recycling process is relatively cheap, provided that the collection of scrap bottles does generate high costs. The profitability of recycling is determined by the price of the final products obtained from recycled PET. Adding high value in the reprocessing step is a requirement for achieving the profitability of PET recycling. In processing, high-quality recyclates must be used: they should contain extremely low amounts of poly(vinyl chloride) (PVC) and glue residue, together below 50 ppm; contain a low concentration of other impurities such as sugar, caramel, soil, cellulose, and polystyrene; possess a high intrinsic viscosity; and have a low concentration of microgels. The recyclates characterized by the previous properties can be obtained by the careful segregation of scrap beverage bottles according to the type of polymer, the removal of labels and glue; cleaning, grinding, and washing, (not necessarily in the indicated sequence); and drying before processing. There should be no regranulation step in recycling as the additional melting can cause excessive degradation by hydrolysis. Such a process of recycling, leading to material with good properties, is described elsewhere.[4]

High value can be added to the products by more sophisticated processing, for example, orientation. One of the most promising products for which the orientation is essential is packaging strap or tape. High-strength straps and tapes are produced from PET by only a few companies (e.g., Signode Co., Vernon, IL). When virgin PET with only a minor addition of recyclate is used, the strength of the tapes is at the level of 410–440 MPa. Other companies use virgin PET with high intrinsic viscosities at a level above 1.0 g/dL. The strength of such tapes reaches 500–550 MPa (e.g., Mosca GmbH, Waldbrunn/Strumpfelbrunn, Germany). The high strength of all these tapes is due to the uniaxial orientation of macromolecular chains resulting from high plastic deformation. In the case of an industrial process for oriented films or straps, the production involves two or three steps: first is cold drawing with constant force, constant speed, or constant tape width; second is the thermal stabilization of

Correspondence to: A. Galeski (andgal@bilbo.cbmm.lodz.pl).
Contract grant sponsor: Poland State Committee for Scientific Research; contract grant number: 7 T08E 052 14.

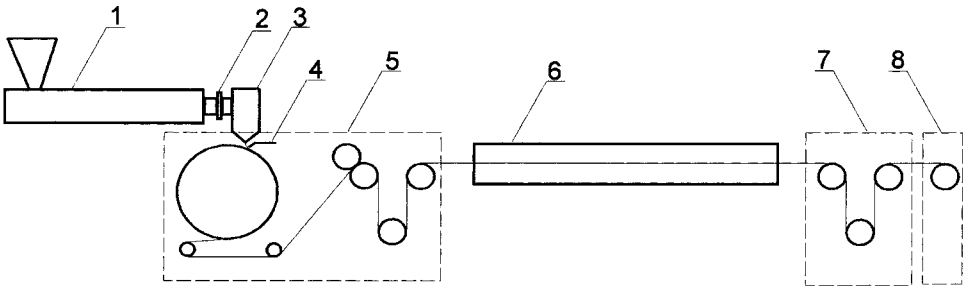

Figure 1 Scheme of the extrusion/stretching line for the drawing of PET tapes: (1) extruder, (2) melt filter, (3) slot extrusion die, (4) air knife, (5) chill roll and slow rolls assembly, (6) heating tunnel, (7) fast rolls assembly, and (8) receiving roll.

tapes or films. In addition, the third step can comprise a transverse drawing for the production of biaxial orientation.

In this research, an effort was made to develop a manufacturing process for high-strength packaging straps from PET recyclate obtained in a previously developed and implemented recycling process of PET beverage bottles.[4] The intrinsic viscosity of individual flakes of such regrinds is usually around 0.8 g/dL; however, remelting always causes a decrease of the intrinsic viscosity of the entire material to 0.4–0.6 g/dL, depending on the impurity level.[5] It is a big challenge to produce high-strength PET tapes from low-viscosity bottle-grade recyclate. High-strength tapes from low-viscosity bottle-grade PET cannot be obtained by drawing to a natural draw ratio because the strength of such tapes is below expectation. We developed a double-drawing process consisting of a second drawing step after free drawing with the natural draw ratio. The second drawing step is performed at a different temperature than the first one, and it is designed to ensure neckless uniform stretching and oriented crystallization of PET tapes.

EXPERIMENTAL

Materials

The source of PET used in this study was postconsumer beverage bottles collected in central Poland. The bottles originated from various producers and were made from various grades of PET. Incidental PVC bottles were separated from the batch by inspection of the bottoms for the absence of injection nods and for whitening of folds when the walls were folded. After the removal of polyethylene caps, the bottles were washed to remove labels, glue, and other impurities. (Labels from some bottles could not be removed by simple washing and rinsing because of the presence of acrylic-based or hot-melt glues. These were removed in the second washing process after shredding.) The bottles were then shredded into flakes 1–8 mm in size. The obtained flakes were carefully washed again with strong agitation; the water was removed in a centrifuge, and the flakes were finally dried and crystallized according to a specially developed heating program in a close air-circulating dryer with molecular sieves as a water absorbent. The final temperature of drying was 170°C. This procedure assured a concentration of PVC below 30 ppm in a 1000 kg batch of PET. The individual flakes of the recyclate obtained in this way were characterized by a mean viscosity of 0.80 g/dL, as determined in a mixture of phenol and 1,1,2,2-tetrachloroethane as a solvent at 23°C. After melting and extruding in the extruder of the injection-molding machine, the intrinsic viscosity of the averaged material dropped to 0.58 g/dL.

Orientation

The flakes of the recycled PET were extruded into tapes of various widths from 10 to 28 mm and various thickness from 0.4 to 1.2 mm; the tapes were then subsequently stretched uniaxially at various temperatures and various deformation rates. The extrusion/stretching was performed on the laboratory line consisting of the single screw extruder (Brabender OHG, Duisburg, Germany, PL2000; $L/D = 25$), the slot extruder head with a controlled opening width and thickness, the chill roll (diameter = 320 mm; temperature controlled with oil flow), a set of slow and fast rolls used for drawing separated by a heating tunnel, and a wind-up roll. The scheme of the extrusion/stretching line is illustrated in Figure 1. The speed of the slow rolls was synchronized with the speed of the chill roll to obtain unoriented tape. The rate of extrusion of tapes was within a range of 50–200 cm/min. The speed of the fast rolls was changed within a range of 50–300 cm/min to control the drawing process. The take-up rolls were synchronized with the fast rolls. The temperature of the chill roll was maintained within a range of 70–80°C with a precision of ±0.5°C. The temperature of the drawing process was varied within a range of 50–160°C. The stretching ratio was measured from the deformation of 10-cm sections between ink marks made on unoriented tapes. The first drawing step was optimized for stability and unifor-

mity of drawing and for the neck positioned at the farther end of the heating tunnel. The obtained oriented tapes were additionally stretched at various conditions in a separate second step with the same stretching line consisting of slow and fast rolls separated by a heating tunnel. The temperature of the second drawing was within a range of 70–160°C. The rate of slow and fast rolls were changed with the same range as in the first drawing step. The second drawing ratio was changed within a range of 1.05–2.0

Measurements

Mechanical properties of the samples were determined from tensile experiments performed at room temperature with an Instron tensile testing machine (model 1114T, Instron Corp., High Wycombe, UK). The crosshead speed was set to 5 cm/min in all tests. This speed assured an initial deformation rate of 100%/min.

Differential scanning calorimetry (DSC) measurements were performed during heating with a TA2000 apparatus (Thermal Analysis, New Castle, DE). The heating rate was 10°C/min.

The density of tapes was determined by floatation in an aqueous solution of a mixture of NaCl and $ZnCl_2$ at 20°C.

The orientation of the crystalline phase of PET in oriented tapes was studied by means of X-ray diffraction with pole figures. A wide-angle X-ray scattering (WAXS) system consisting of a computer-controlled pole-figure device associated with a wide-angle goniometer coupled to a sealed tube X-ray generator operating at 30 kV and 30 mA was used in this study. The X-ray beam consisted of CuKα radiation filtered by a Ni filter and electronically. For pole-figure data acquisition, we used the procedure elaborated earlier. The details of pole-figure determination procedure were described elsewhere.[6]

The following diffraction reflections from triclinic crystal structure of PET were analyzed for the construction of pole figures: (010), (100), and $(\bar{1}05)$[7] found in our case at the diffraction angles $2\theta = 17.1$, 25.1, and 42.2, respectively. The slit system of the diffractometer was always selected to measure the integral intensity of the appropriate diffraction peak. The necessary corrections for background scattering and sample absorption were introduced to raw data. The pole-figure plots were generated by the POD program, a part of the popLA package (Los Alamos National Laboratory, Los Alamos, New Mexico). For every plot, the data were normalized to the random distribution density.

Dynamic mechanical properties of the tapes were measured by means of a Rheometric MkIII dynamic mechanical thermal analysis (DMTA; Rheometric Scientific, Inc., Epsom, UK) apparatus in a double cantilever bending mode at 1 Hz as a function of temperature in a range from −120 to 150°C at 2 deg/min.

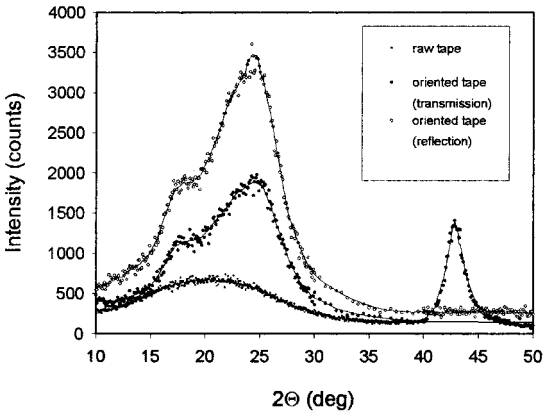

Figure 2 Typical 2θ X-ray diffraction spectra of extruded undrawn and drawn tapes obtained from scrap PET.

RESULTS AND DISCUSSION

Unoriented tape

The width and the thickness of extruded tapes were set by the width and the thickness of the slit of the extruder head. However, the width and thickness of extruded tapes could also be adjusted by the take-up speed of the chill roll. With a slot of 1×35 mm, the width of the extruded tape could be varied from 6 to 28 mm, whereas the thickness could be varied from 0.4 to 1.2 mm, depending on the speed of the chill roll. A good thermal contact with the chill roll was achieved by the "air knife": a slit through which the ambient air was blown at the extruded tape and which pressed the tape against the chill roll. Unoriented extruded tapes obtained with a chill roll temperature of 80°C were transparent, flexible, and resistant to tearing and did not break when folded tightly. As follows from the wide angle X-ray diffraction, the tapes were highly amorphous. Figure 2 shows the typical 2θ X-ray diffraction spectrum. Only the broad amorphous halo with the peak at around $2\theta = 20°$ can be distinguished, whereas no typical sharp diffraction peaks from crystalline phase can be distinguished.

The DSC run of the unoriented tape obtained from recycled PET exhibited a glass-transition temperature (T_g) at 77°C; the cold crystallization had a peak around 131°C with the onset at 125°C, the tail extended over several 10s of degrees up to 210°C, and the latent heat of fusion was 34 J/g. At higher temperatures, the melting of crystals was seen with a peak at 251°C, and the heat of melting was 41 J/g. A difference at the level of 7 J/g between the heat of fusion in cold crystallization and heat of melting accounted for the small

TABLE I
Tensile Properties of Unoriented PET Tape

Temperature (°C)	Tensile modulus (MPa)	Yield stress (MPa)	Stress at break (MPa)	Elongation to break (%)
20	1170	58	50	420
95	2.95	1.13	16.7	1020

amount of crystals that were formed during cooling on a chill roll.

The mechanical properties of unoriented tapes obtained from recycled PET were determined in tension at two temperatures: 20 and 95°C, with a drawing rate of 100 mm/min and a gauge length of the samples of 100 mm. The data are collected in Table I. The tensile parameters at 20°C were similar for those usually obtained for virgin PET of low crystallinity with only slightly lower yield stress. The low tensile modulus, low yield stress, and high elongation at break observed at 95°C [i.e., above T_g (77°C) but below the cold crystallization range (onset at 125°C)] confirmed that the tapes had a very low crystallinity.

First drawing step

Initial experiments of the orientation of PET tapes were performed on an Instron machine at various temperatures. The orientation process should be carried out at the temperature around or slightly below T_g. Above T_g, strong crystallization enhanced by orientation takes place: at 200°C the time of crystallization is around 0.1 s only. The crystalline phase is less susceptible to orientation than the amorphous phase at temperatures above or at T_g; hence, the inhomogeneities due to the presence of crystallites reduce the elongation and the molecular orientation in PET tapes. Therefore, the tapes extruded on the chill roll should have had the lowest possible crystallinity to assure high drawability in the orientation step. The drawing needed to be performed at a temperature below the onset of the cold crystallization temperature, that is, below 125°C, at which PET exhibits a drastic decrease of yield stress and the cold crystallization sets in.

Pilot extrusion and stretching at 90°C on the extrusion/stretching line demonstrated several undesirable effects: the process of drawing was unstable and the neck region was traveling within heated tunnel, at one moment being at its entrance and in a while moving to its center. The stretching proceeded then at different temperatures, resulting in a nonuniform tape. Typical mechanical data of the tapes with a stretching ratio of 7 were tensile modulus = 1.84 GPa, tensile strength = 140 MPa, and elongation at break = 60–70%. In a series of experiments, the optimal drawing temperature was found to be 75–77°C. The requirements were the stability of the stretching process, stability of the tape width and thickness, high tensile mechanical parameters, resistance to longitudinal cleavage, and resistance to fibrillation. At 75–77°C, it was relatively easy to set the drawing rate and the drawing ratio at such level that the stretched tape became uniform with the natural draw ratio in a range from 4 to 4.3. The take-up velocity was slightly below 3 m/min. The parameters for that tape are listed in Table II. The strength of the tape was rather high, exceeding 300 MPa, whereas the elongation at break was at a level of 30–40 %, the longitudinal cleavage was difficult, and the tape remained transparent. These parameters fulfilled easily the standards for polypropylene packaging tapes, for which the mechanical parameters are also listed in Table II. The mechanical data for the single-stretched PET tapes were comparable to the polypropylene tapes (Cyklop GmbH, Cologne, Germany), except for higher elongation to break.

The natural draw ratio of these tapes was rather low, and any effort to increase it by increasing the speed of fast rolls resulted in the travel of the neck

TABLE II
Mechanical Parameters of PET Tapes and Comparison with Polypropylene Tapes

	Recycled PET				Virgin PET, bottle grade (Connect)		
	λ = 4.0–4.3, Single drawn	λ = 5.0, Double drawn	λ = 5.6, Double drawn	λ = 6.0, Double drawn	λ = 4.0 then 5.6, Double drawn	PET Tenax (Signode)	Isotactic polypropylene (Cyklop)
Tensile strength (MPa)	300–350	400	550	>600	680–700	410–440	280
Elongation at break (%)	30–40	>15	10–11	<9	10–12	12–15	13
Transparency	Yes	Yes	Yes	Yes	Yes	Yes	No
Longitudinal splitting	No	No	No	Yes	No	No	Yes

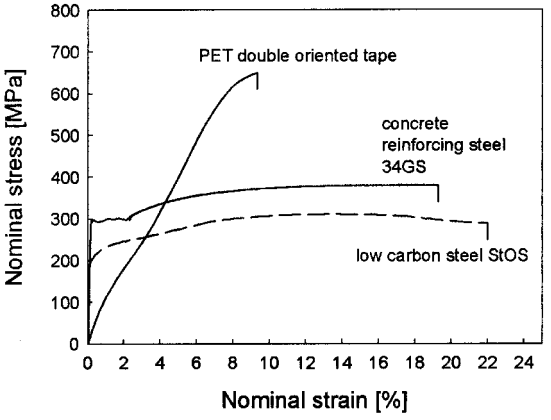

Figure 3 Stress–strain curve for double-oriented PET tape. The stress–strain curves of low carbon steel (StOS) used for packaging and of concrete reinforcing steel (34GS) are also presented for comparison.

region to the entrance of the heating tunnel, where the temperature assumed by the tape was much lower. This was an undesired situation because at a lower temperature, the drawing of the tape involved cavitation associated with significant whitening and a marked decrease of the mechanical strength.

Second drawing step

To increase the draw ratio, the tapes were further stretched in the separate second step with identical system of slow and fast rolls. The second stretching of tapes proceeded without necking and uniformly over the entire tape length enclosed in the heating tunnel. The stretching ratio could now be set at various levels up to a total ratio of 7. In a series of experiments, we found that the optimum temperature of drawing was 125–130°C with a rate of 3 m/min. Again, the requirements were the stability of the stretching process, stability of the tape width and thickness, high tensile mechanical parameters, resistance to longitudinal cleavage, and resistance to fibrillation.

The mechanical parameters characterizing the tapes after the second additional stretching are also presented in Table II. These data show that the strength of the tape increased and the elongation at break decreased, whereas the total draw ratio increased. The tape drawn to the total draw ratio of 6 had tensile strengths well above 600 MPa. The stress–strain curve for double-oriented PET tape is shown in Figure 3. The initial slope of 12 GPa was linear up to a stress of 130 MPa and then decreased to 7.5 GPa. This region extended to a stress of roughly 550 MPa, above which the yielding process set in. The fracture occurred at 670 MPa. For comparison, the stress–strain curves of low-carbon steel (StOS) used for steel packaging tapes and of concrete reinforcing steel (34GS) are also presented in Figure 3. The PET tape was much stronger than both steel materials and had a lower tensile modulus and lower elongation to break.

The obtained tapes, at all applied draw ratios, were transparent and resistant to longitudinal cleavage, except for those with a draw ratio higher than 6. The data presented in Table II suggest that the tape deformed to a total draw ratio of 5.6 exhibited the best balance of mechanical and overall properties for the application as a packaging tape with high strength and low elongation at break. The tapes obtained with a draw ratio of 6 had higher tensile strength yet showed undesirable longitudinal cleavage and some tendency to fibrillation.

In the industrial implementation of the sequential drawing process (Connect Co., Sokolow Malopolski, Poland) a take-up rate of 120 m/min was achieved with other parameters, such as tape temperatures and draw ratios during both drawing steps, not differing significantly from those in the laboratory set up. The basic parameters for such tapes are presented also in Table II.

Crystallinity

All oriented tapes exhibited some degree of crystallinity generated during stretching, which could be detected either by density measurements or by wide angle X-ray diffraction.

Table III presents the density data obtained by volumetric measurements. We recalculated the density to crystallinity degree, assuming the density of the amorphous phase of PET was 1.335 g/cm^3 [8] and the density of the crystalline phase was 1.455 g/cm^3.[9] The unoriented tape was almost amorphous (the crystallinity degree was less than 3%). This conclusion was also supported by the wide angle X-ray diffraction already presented in Figure 2, where only an amorphous halo and no crystalline peaks were seen. The very low crystallinity the level of 5% was also estimated from DSC data [as calculated from the difference between the heat of melting and the heat of fusion of cold crystallization (with the heat of fusion taken at 140.1 J/g[10])].

TABLE III
Density and Crystallinity Degree of PET–Drawn Tapes Determined Based on Density

Tape	Density (g/cm^3)	Crystallinity (%)
Unoriented	1.3383	2.75
Single drawing (λ = 4.3)	1.3745	26.76
Double drawing (λ = 5.6)	1.3770	24.80
Double drawing (λ = 6.0)	1.3750	26.65

TABLE IV
Thermal Parameters of Unoriented and Oriented Tapes from Recycled PET Obtained at a Heating Rate of 10°C/min

	T_g(°C)	T_c peak (°C)	ΔH_c (J/g)	T_m onset (°C)	T_m peak (°C)	T_{m1} peak (°C)	ΔH_m (J/g)	Crystallinity[a] (%)
Unoriented tape	77.0	130.7	34.1	237.2	251.6	—	41.1	5.0
Tape, single drawn to 4.3 ×	69.3	100.1	10.2	240.0	246.8	252.1	54.8	31.8
Tape, double drawn 5.6 ×	63.4	104.3	12.7	243.0	248.2	252.0	57.3	31.8
Tape, double drawn 6.0 ×	63.9	93.1	12.6	241.7	247.0	252.0	57.35	31.9
Unoriented tape, annealed for 15 min at 150°C	83.3	138.9	2.8	237.9	252.0	—	41.4	27.6

T_c, cold crystallization temperature; ΔH_c, heat of fusion of cold crystallization; T_m, melting temperature of the first melting peak; T_{m1}, melting temperature of the second melting peak.

[a]Calculated as the difference between the heat of melting and the heat of fusion of cold crystallization. The heat of fusion of 100% crystalline material was assumed to be 140.1 J/g after ref. 10.

The tape drawn to the ratio of 4.3 exhibited a crystallinity degree around 33% (density estimated). Crystallinity development was also detected from the crystalline peaks observed by wide angle X-ray diffraction (see Fig. 2). The crystal orientation was already seen from the meridional position of ($\bar{1}05$) reflex. As the tape was drawn in the second drawing step, the crystallinity remained almost constant at 35% at a draw ratio of 5.6 and 33.3% at a draw ratio of 6.0.

The previous data were confirmed by DSC measurements, as seen in Table IV. DSC data also demonstrated that the unoriented tape was capable of strong cold crystallization during heating with a peak at 134.9°C. Annealing of the unoriented tape at 150°C for 15 min suppresses the ability to further cold crystallization. The oriented tapes also exhibited a lowered capability of cold crystallization, all of them at a level of 10–12 J/g, which corresponded to 7–8% crystallinity. The melting peak of the unoriented tape was at 251.2°C, whereas all oriented tapes showed double melting peaks: the first maximum at 246–248°C and the second at 252°C. The relative heights of those peaks suggest that the 252°C peak was due to the melting of crystals formed in strain-induced crystallization, whereas the 246–248°C peak was the melting of cold-crystallized crystals formed during DSC scans. The growth of the later crystals was defective and led to small sizes due to constraints from existing strain-induced crystals. The peak of cold crystallization was significantly shifted toward lower temperatures in all drawn samples as compared to the unoriented sample. The crystallinity degrees calculated from the difference of the heat of melting and the heat of fusion of cold crystallization (Table IV) agreed well with the crystallinities determined from the density measurements (Table III).

The double-drawn tapes were subjected to a high temperature at 130°C during second drawing step; nonetheless, later, due to relaxation with free ends, the tapes were able to further limit cold crystallization during DSC heating scan beginning with the temperature slightly above T_g.

Texture

The texture of oriented PET tapes was studied by means of X-ray diffraction with the construction of pole figures. The 2 cm long pieces of the tapes were arranged on the plane to obtain approximately 4-cm^2 samples. In 2θ scans, the reflections at 17.1, 25.1, and 42.2° corresponded to (010), (100), and ($\bar{1}05$) reflections from triclinic crystals, respectively. The triclinic crystallographic form of PET has the following parameters: $a = 4.56$ Å, $b = 5.94$ Å, $c = 10.75$ Å, $\alpha = 98.5°$, $\beta = 118°$ and $\gamma = 112°$.[11] The c axis of the unit cell is parallel to the macromolecular chain axis, whereas the plane of phenyl rings is nearly perpendicular to a axis. From X-ray diffraction, it is possible to obtain information about orientation of particular crystallographic planes and not directly about the orientation of unit cell axes. Nevertheless, the information about orientation of phenyl rings can be estimated from the position of (100) reflection because the normal to this plane is tilted by approximately 19° with respect to the normal to the phenyl ring plane. The position of ($\bar{1}05$) reflection delivers the information on the orientation of macromolecular chains because the c axis is tilted by only 9.8° with respect to the normal to ($\bar{1}05$) plane. At first approximation, the deviations of (100) and ($\bar{1}05$) reflections from the a and the c axes can be disregarded.[12,13] In addition to the previous three integral pole figures for crystallographic peaks, the "height pole figure" of the amorphous phase was constructed from scattering data collected at $2\theta = 19.5°$. At this angle, there was a maximum of the amorphous halo of unoriented PET. Besides, this region of diffraction angles was relatively free of crystalline diffraction peaks. The pole figure for the amorphous halo was constructed in the past for polyethylene and for polyamide 6 to gain the information about the orientation of the amorphous phase.[14,15] In such a case, the amorphous halo was treated as a (100) reflection from pseudohexagonal close packing of the amorphous phase. Clustering of these reflections gave the information about orienta-

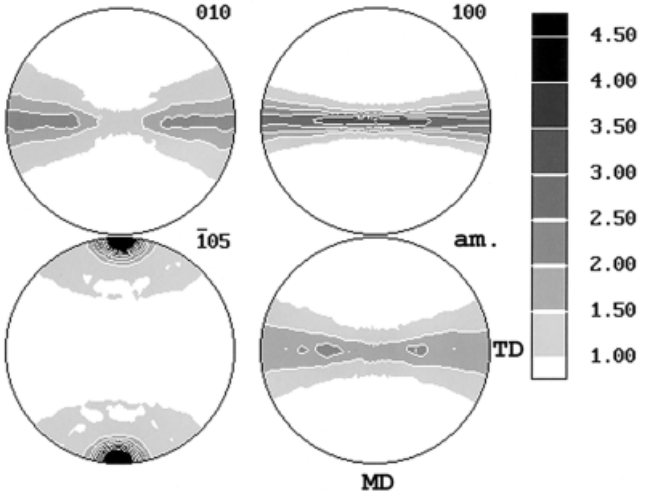

Figure 4 Set of pole figures for PET tapes oriented in a single step to the draw ratio of 4.3.

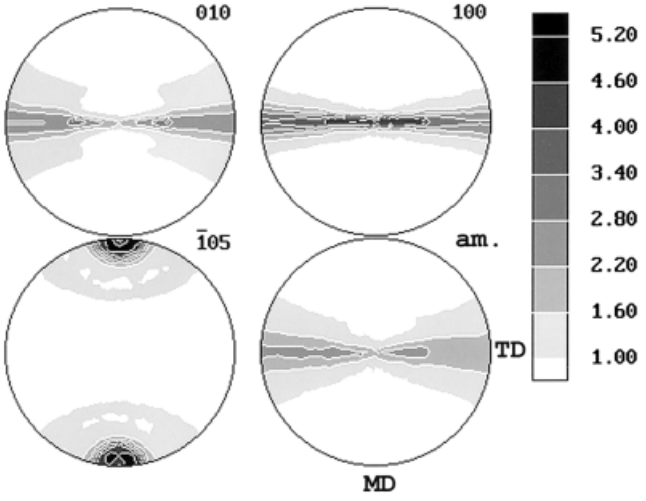

Figure 5 Set of pole figures for PET tapes oriented in two steps to the draw ratio of 5.6.

tion of those chain fragments that are in the amorphous state. The pole figures presented in this article contain only limited and approximate information on amorphous orientation because they were constructed from the data of the intensity of scattering at the maximum of the amorphous halo, instead of integral intensity.

Figure 4(a–d) shows the set of pole figures for the tapes oriented in a single step to a draw ratio of 4.3. The pole figures indicate the formation of a strong texture produced by stretching: macromolecular chains in crystals were preferentially oriented along the drawing direction as was judged from the clustering of ($\bar{1}05$) normals. Normals to (100) and (010) planes of crystals were concentrated in two distinct populations tilted at some acute angles in the equatorial plane with respect to the flat tape surface, indicating quasi single-crystal texture. Because the initial unoriented material was nearly amorphous, the origin of texture was mostly the strain-induced crystallization and, to a lesser extent, the plastic deformation and rotation of newly formed crystals.

The ratio of thicknesses of the initial unoriented tape to oriented tape was 2.31, whereas width ratio was only 1.50. This suggests that the drawing was anisotropic in the plane perpendicular to the drawing direction because of constraints due to large width of the tape as compared to its thickness and constraints due to friction along the drawing rolls.

The pole figure constructed for the heights of the amorphous halo [Fig. 4(d)] also indicated a high orientation of chains in the amorphous phase along drawing direction. There was a trace of anisotropic packing of chains of the amorphous phase in the plane perpendicular to the drawing direction.

Almost no new crystals were formed in the second step of drawing as it followed from the density (Table III) and DSC data (Table IV). Both sets of data indicated that there was no further increase in the crystallinity degree in the second step of drawing.

In the set of pole figures obtained for the tape oriented in a two-step process to a draw ratio of 4.3 and 5.6 [see Fig. 5(a–d)], the crystals formed in the first drawing were subjected to strong load; however, their orientation with macromolecular chains along the drawing direction prevented generation of significant shear within possible glide planes and directions that were observed in PET:[16] the easiest (100)[001] chain slip and (100)[010] transverse slip. There was no evidence of other possible slip: (010)[001] chain slip. Only a fraction of less perfectly oriented crystals became better aligned with their chain axes along the drawing direction due to (100)[001] and (100)[010] slip systems. This led to some sharpening of the texture in the orthogonal plane: stronger clustering of (100) normals around $\alpha \approx 30°$ was seen, whereas (010) normals were

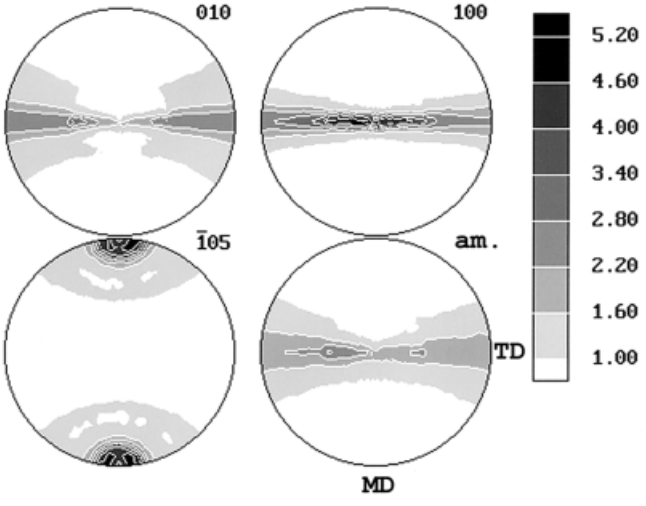

Figure 6 Set of pole figures for PET tapes oriented in two steps to the draw ratio of 6.0.

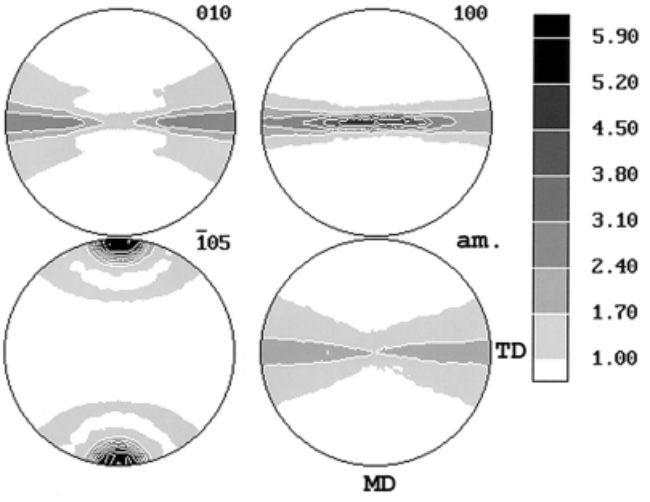

Figure 7 Set of pole figures for PET tapes oriented in two steps to the draw ratio of 6.0 and then annealed with fixed ends at 90°C for 15 min.

positioned in a wider range of angles from 25 to 90°. This widening followed from the fact that if the (100) texture was well defined in the orthogonal plane, there were four possible positions of triclinic unit cell of PET, hence four positions of (010) normals, all lying and overlapping in the orthogonal plane. In Figure 5(a), which presents the (010) pole figure, those four clustering regions are faintly visible.

As the drawing ratio was increased to total 6, the ($\bar{1}05$) texture became very sharp, as is shown in Figure 6(a–d). The cluster of ($\bar{1}05$) normals was clearly split into two sharp maxima, displaced by approximately 10°. The splitting resulted from the tilt angle of ($\bar{1}05$) normal with respect to the macromolecular chain axis in triclinic crystals and indicated extraordinary sharp orientation of macromolecular chains along the drawing direction.

The pole figures of (010) and (100) normals showed more fibrous texture, especially the (010) pole figure, which lost the four-point clustering in the orthogonal plane. It is most probable that, besides (100)[001] chain slip, similar to the sample with a draw ratio of 5.6, the (100)[010] transverse slip was also active. The (100)[010] transverse slip set in at later stages of plastic deformation, due to higher critical resolved shear stress, and also controlled the orientation of crystal structure in the plane orthogonal to the flow direction.

The sample of the tape double drawn to a total draw ratio of 6 was subjected to annealing with fixed ends at 90°C for 15 min. Such tape showed further sharpening of ($\bar{1}05$) texture [see Fig. 7(a–d)], as was noticed from the pronounced split of the clustering of ($\bar{1}05$) normal. Such splitting was already observed for double-drawn tapes to a total draw ratio of 5.6 and 6. The pole figures for (010) and (100) normals showed a tendency to some relaxation and, hence, evolved toward a more fibrous texture.

The annealing also caused a deterioration of the amorphous phase orientation orthogonal to the draw direction as compared to unannealed samples, as is shown in Figure 7(d).

The tape with the best overall properties (stretching ratio = 5.6) was tested for thermal stability by annealing with free ends from room temperature to 90°C. The mechanical data and the shrinkage due to thermal treatment are presented in Table V. The thermal shrinkage was limited to 8% only, even if the tape was annealed at 90°C, that is, above T_g of unoriented recycled PET (77°C). The strength at room temperature of the annealed samples decreased moderately, but it was always above 450 MPa. The elongation at break increased with the increase of annealing temperature, but it was always in the accepted range, well below 45%, if the tape was intended to be used as a packaging strap. It was apparent that the crystallinity level was sufficient to immobilize the material of oriented tape against the relaxation above T_g. to a large extent.

Dynamic mechanical properties

In Figure 8(a,b), the DMTA data for unoriented and oriented tapes are presented. In addition the DMTA, data for the unoriented PET sample annealed at 150°C are plotted. The unoriented sample exhibited the α relaxation T_g at 75–77°C with a significant tan δ peak. Further increases in temperature resulted in cold crystallization and a hardening of the sample with onset at 117°C. These observations were confirmed by associated DSC results (see Table IV). The sample that was annealed at 150°C also exhibited a T_g at 75–77°C; however, it already showed considerable stiffness due to the presence of crystals formed on annealing. Only limited cold crystallization was observed in this sample. In oriented samples, that α transition was significantly depressed: single-oriented tape (draw ratio = 4.3) showed only slight decreases in modulus above 110°C, although the T_g of these sample decreased to 65–70°C. This effect could be explained by cold crystallization, which set in immediately after T_g was

TABLE V
Shrinkage and Mechanical Properties of the PET Tape Double Drawn Annealed at Various Temperatures

	As drawn	48 h at 23°C	35°C	40°C	50°C	60°C	70°C	90°C
Shrinkage (%)	0	−1	−1.3	−1.4	−2.5	−4.3	−4.7	−8
Strength (MPa)	550	545	480	470	470	465	480	460
Elongation at break (%)	10	10	13	13	17	22	19	24

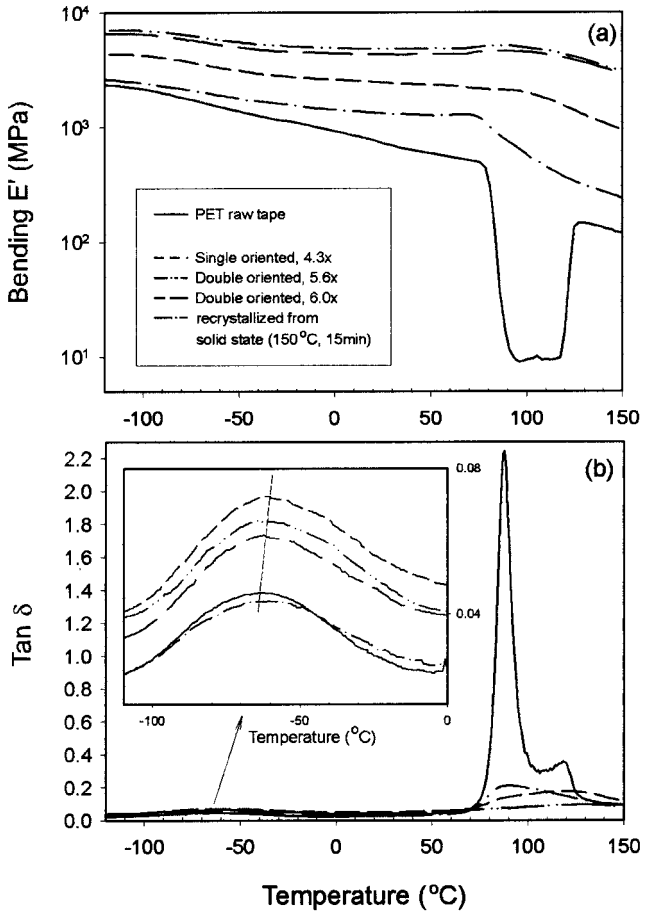

Figure 8 (a) E'-bending storage modulus and (b) tan δ for unoriented and oriented PET tapes in one and two steps of drawing. The data for the unoriented PET tape annealed at 150°C for 15 min is also presented. The insert in Figure 10(b) is an enlargement of the β relaxation range.

reached (compare Table IV). The transition in double-oriented tapes was pronounced very little [see the insert in Fig. 8(b)].

The β transition covered a range of temperature, with a maximum around −64°C for unoriented PET tape. It became slightly less emphasized for the sample that was annealed at 150°C, whereas for oriented samples, the β transition was more pronounced than for row tape: for single-oriented tape, the β peak in tan δ was the highest and decreased for double-oriented tapes. It decreased further as the draw ratio increased [see the second insert in Fig. 8(b)].

The β secondary relaxation process appears usually in PET as a weak and broad maximum of tan δ with a peak near −65°C. It has been postulated[17] that the β process consists of two different components due to the motion of carbonyl groups (low temperature part) and phenyl ring flips (high temperature part). In fact, in our data, two components of the relaxation peak could be distinguished. In Figure 9, the exemplary deconvolution of these two contributions for the β relaxation process is depicted. The fit to the experimental points made with two Gaussian curves was very good. The fitted data for these two components for all tapes studied are collected in Table VI. In unoriented PET tape, the low temperature component had a maximum at −81°C with an area of 0.41. In cold-crystallized PET, this component was slightly lower due to dumping of carbonyl group motion in crystals. As the orientation increased, this process intensified; apparently such motion can be more intense due to some cooperativity of chain fragments motion, which are arranged parallel in the oriented amorphous phase of PET. The temperature of the maximum of β_1 process shifted toward higher temperature as the increasing orientation was imposed on PET, and the state of orientation was fixed by strain-induced crystallization.

Similar to the β_1 relaxation, the β_2 process also shifted toward higher temperatures with the increase in crystallinity and orientation; however, the intensity of this process was reduced due to crystallinity. On the other hand, the orientation in the single-step produced highly oriented crystalline and amorphous material, but the amorphous phase was not yet very much strained, as follows from a still low modulus, high elongation to yield, and high elongation to break. Hence, for the single-oriented tape, the β_2 process, which concerns the flips of phenyl rings in the backbone chains, was more intense than in unoriented raw or annealed samples. As the orientation and strain of tie molecules in the amorphous phase of double-oriented tapes increased, this process became less intense. Because the β_2 relaxation was responsible for the brittle behavior of PET at a low temperatures (−20°C), the decrease of β_2 relaxation intensity in double-oriented tapes was beneficial.

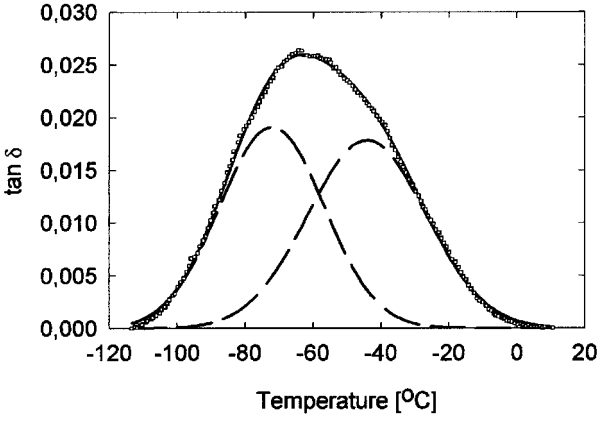

Figure 9 Exemplary deconvolution of the β relaxation peak of PET-drawn tape (single-step drawing, draw ratio = 4.3) into two contributions: from the motion of carbonyl groups (low-temperature part) and phenyl rings flip (higher temperature part).

TABLE VI
β Relaxation Processes of PET Tapes

Sample	β relaxation		β_1 component		β_2 component	
	Peak temperature (°C)	Intensity (a.u.)	Peak temperature (°C)	Intensity (a.u.)	Peak temperature (°C)	Intensity (a.u.)
Unoriented tape	−64.0	1.30	−81.4	0.41	−55.4	0.89
Annealed unoriented tape	−62.2	1.04	−79.8	0.37	−52.2	0.67
Single-oriented tape, 4.3×	−59.4	1.64	−74.1	0.65	−47.8	0.99
Double-oriented tape, 5.6×	−60.4	1.54	−72.5	0.79	−44.9	0.75
Double-oriented tape, 6.0×	−58.6	1.51	−71.7	0.76	−43.6	0.74

β_1 = Motions of carbonyl groups; β_2 = phenyl ring flips.

CONCLUSIONS

Postconsumer PET beverage bottles can be used for the production of ultrastrong PET tapes suitable for packaging straps. The developed two-step continuous drawing process assures that the tapes can be produced from bottle-grade PET with intrinsic viscosities of 0.7–0.8 g/dL instead of tape-grade material with intrinsic viscosities above 1.0 g/dL. The strength of such tapes, if the drawing process is set correctly, approaches 700 MPa: in other reports concerning stretching of short pieces of tapes, the achievable strength rarely exceeded 700 MPa (e.g., ref. 18, where the zone heated multistep stretching was described).

Despite a decrease in the viscosity of recycled PET due to impurities, the tapes were extruded and drawn in a continuous manner with no problems. After double drawing, the molecular orientation was very high, as revealed by X-ray pole figures: the concentration of $(\bar{1}05)$ normals was split into two populations, indicating almost perfect alignment of chain axes in crystals along the drawing direction.

A strong texture was produced during the first stretching step: macromolecular chains in crystals were preferentially oriented along the drawing direction. Also, the amorphous halo in WAXS experiments indicated high orientation of chains in the amorphous phase along the drawing direction. Because the initial unoriented material was nearly amorphous, the origin of texture was mostly the strain-induced crystallization and, to a lesser extent, plastic deformation and rotation of newly formed crystals. The quasi single-crystal texture was the result of anisotropic strain developed in the plane perpendicular to the drawing direction because of constraints due to the large width of the tape as compared to its thickness and constraints due to friction along the drawing rolls.

Plastic deformation mechanisms of crystals were activated in the second step of drawing: (100)[001] chain slip and (100)[010] transverse slip were recognized on inspection of WAXS pole figures.

The strength of drawn tapes annealed with free ends decreased slightly, whereas the elongation at break increased with increases in annealing temperature. It was apparent that the crystallinity developed during drawing was sufficient to immobilize the material of oriented tape against the relaxation, which preserved the good mechanical properties of the tape.

The process of double drawing PET for the production of superstrength tapes can be easily implemented on an industrial scale

References

1. Scheirs, J. Polymer Recycling; Wiley: Chichester, England, 1998, p 119.
2. (To AKW GmbH; Ropertz, G.; Kaniut, P.). Ger. Pat. DE 37 28 558 A1 (1987).
3. (To Herbold GmbH; Beyer, S.). Ger. Pat. DE 38 31 023 A1 (1988).
4. (To Polish Academy of Sciences; Galeski, A.; Morawiec, J.; Bartczak, Z.). Pol. Pat. Appl. P-317475 (1996).
5. Pawlak, A.; Pluta, M.; Morawiec, J.; Galeski, A.; Pracella, M. Eur Polym J 2000, 36, 1875.
6. Bartczak, Z.; Krasnikova, N. P.; Galeski, A. J Appl Polym Sci 1996, 62, 167.
7. Roeber, S.; Gehrke, R.; Zahmann, H. G. Mater Res Soc Symp Proc 1987, 79, 205.
8. Thompson, A. B.; Woods, D. W. Nature 1955, 176, 78.
9. de Daubeny, R.; Bunn, C. W.; Brown, C. J. Proc Roy Soc (London) A 1954, 226, 531.
10. van Krevelen, D. W. In Properties of Polymers (3rd ed.); Wiley: New York, 1990.
11. Daubeny, R. P.; Bunn, C. W.; Brown, J. C. Proc Roy Soc (London) A 1954, 226, 531.
12. Faisant de Champchesnel, J. B.; Bower, D. I.; Ward, I. M.; Tassin, J. F.; Lorentz, G. Polymer 1993, 34, 3763.
13. Lapersonne, P.; Tassin, J.; Monnerie, L. Polymer 1991, 32, 3331.
14. Galeski, A.; Argon, A. S.; Cohen, R. E. Macromolecules 1991, 24, 3945.
15. Galeski, A.; Bartczak, Z.; Argon, A. S.; Cohen, R. E. Macromolecules 1992, 25, 5707.
16. Bellare, A.; Argon, A. S.; Cohen, R. E. Polymer 1993, 34, 1393.
17. Maxwell, A. S.; Monnerie, L.; Ward, I. M. Polymer 1998, 39, 6851.
18. Goeschel, U. Acta Polym 1989, 40, 23.